Design Considerations of MIMO Antennas for Mobile Phones

M. Usman, R. A. Abd-Alhameed, and P. S. Excell

Mobile and Satellite Communications Research Centre
Richmond Road, University of Bradford, Bradford, West Yorkshire, BD7 1DP, UK

Abstract— The paper presents a new modeling and design concept of antennas using polarization diversity of 2×2 and 3×3 Multiple Input Multiple Outputs (MIMO) system that is proposed for future mobile handsets. The channel capacity is investigated and discussed over Raleigh fading channel and compared to a linear/planner antenna array MIMO channel. The capacity is also discussed over three types of power azimuth spectrums. The results are compared to the constraints capacity limits in which the maximum capacity observed.

1. INTRODUCTION

MIMO for short, which stands for Multiple Input, Multiple Output systems are theoretically able to provide increased throughput, and better error performance than traditional systems [1–5]. The particular aspect that is used by MIMO systems is called *Multi*-Path propagation [2, 5]. This effect occurs when the radio signals sent from the transmitter bounce off intermediate objects before reaching the receiver. Some of these reflected signals may travel along entirely separate paths, and even reach the receiver at different times. Currently, there are a number of MIMO applications, development platforms, and tools that are showing great promise in the quest for wireless systems with higher bandwidth and greater capabilities. The major advantage of MIMO technology is the digital beam forming, which is now making its way out of research laboratories and into real-world applications with great speed. Spatial corrrelation using polarization issues for MIMO applications has great interest since the size of the actual radiating elements can be reduced [6–12]. This study has great advantages if a MIMO system needs to be implemented on a mobile handset. This paper will consider the spatial polarization technique and how this technique can improve the capacity of the system. A MIMO system of 2×2 and 3×3 elements will be considered for implementations on mobile handsets. This will be discussed under Raleigh fading channel and the results will be compared to linear or planer array antenna MIMO system. More over different types of power azimuth spectrums will be considered for system evaluation.

2. SUMMERY OF THE METHOD

For a system having N transmitters and N receivers the channel capacity can be given by [1];

$$C = E \log_2 \left| \left(I + \frac{P_t}{n_t \sigma} H H^* \right) \right| \tag{1}$$

where I is the identity matrix of $n_r \times n_r$ dimensions. P_t is the total average transmitted power. σ is the variance of the noise power, H is the channel transfer matrix of size $n_r \times n_t$. $E()$ is the expectation average and '$*$' is the conjugate transpose operation.

If the receiver and transmitter spatial matrixes are none then the matrix HH^* can be rewritten as follows:

$$HH^* = W_r G_w W_t^* \tag{2}$$

where W_r and W_t are the spatial matrices of the receiver and transmitter respectively. G_w is the matrix that defines the channel properties. For example the elements of the G_w matrix in Raleigh fading channel are complex guassian distributed elements. Since the space availability on the transmitter side then the spatial matrix of the transmitter for maximum channel capacity can be given as an identity matrix. Therefore Eq. (2) can be reduced to the following:

$$HH^* = W_r G_w \tag{3}$$

The elements of the spatial matrix W_r can be stated as follows:

$$W_{r_{i,j}} = \frac{\oint_s (E_{ai} \cdot E_i)(E_{aj} \cdot E_i)^* d\Omega}{\sigma_1 \sigma_2} \tag{4}$$

where

$$\sigma_1 = \oint_s (E_{ai} \cdot E_i)^2 d\Omega \tag{5}$$

$$\sigma_2 = \oint_s |E_{aj} \cdot E_i|^2 d\Omega \tag{6}$$

$$\oint_s = \int_{\phi 1}^{\phi 2} \int_{\theta 1}^{\theta 2} \tag{7}$$

$$d\Omega = \sin\theta \; d_\theta d_\phi \tag{8}$$

and E_a is the electric field of the radiating element. E_i is the incident field on the receiver side.

Using polarization concept we assume that there were three dipoles collocated over the z axis and centered at origin point as shown in Figure 1. We restrict our study to three radiating elements and in which the mutual coupling are ignored and they will located with respect to the elevation angle (it is the polarization angle in our case). We reduced the complicity of the method implementation by using short diploes in which the field can be easily stated (as example for a short dipole oriented in the z axis the total field is $E_\theta = \sin\theta$).

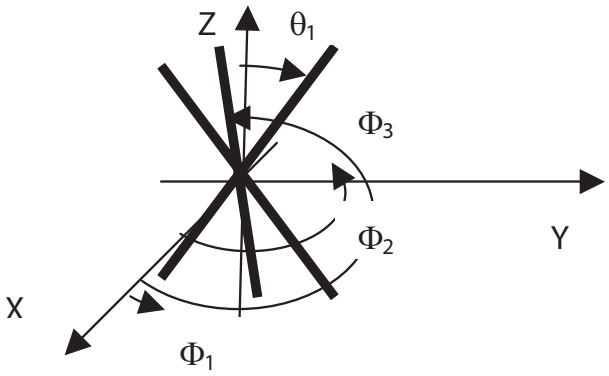

Figure 1: Basic antenna geometry.

The direction of a dipole oriented in θ_d and ϕ_d can be expressed as follows:

$$\hat{\mathbf{d}} = \sin\theta_d \cos\phi_d \hat{\mathbf{a}}_x + \sin\theta_d \sin\phi_d \hat{\mathbf{a}}_y + \cos\theta_d \hat{\mathbf{a}}_z \tag{9}$$

Then the radiated field of this dipole can be given as follows:

$$E_a = E_{\theta a} \hat{\mathbf{a}}_\theta + E_\phi \hat{\mathbf{a}}_{\phi a} \tag{10}$$

where

$$E_\theta(\theta, \phi) = \hat{\mathbf{d}} \cdot \hat{\mathbf{u}}_\theta \tag{11}$$

$$E_\phi(\theta, \phi) = \hat{\mathbf{d}} \cdot \hat{\mathbf{u}}_\phi \tag{12}$$

$$\hat{\mathbf{u}}_\theta = \cos\theta \cos\phi \hat{\mathbf{a}}_x + \cos\theta \sin\phi \hat{\mathbf{a}}_y + \sin\theta \hat{\mathbf{a}}_z \tag{13}$$

and

$$\hat{\mathbf{u}}_\phi = -\sin\phi \hat{\mathbf{a}}_x + \cos\phi \hat{\mathbf{a}}_y \tag{14}$$

3. SIMULATION AND MEASUREMENT RESULTS

If the signal to noise ratio is high then the channel capacity can be given by [5]:

$$C = \sum_{i=1}^{n} \left(I + \frac{P}{n_T \sigma} \lambda_i \right) \tag{15}$$

where λ_i for $i = 1, 2, 3$ are the eign values of the matrix given in Eq. (3). However, the channel capacity is also computed for comparison using Eq. (1). The incident fields are assumed to have uniform distribution over the range 0 to 2π for azimuth angle ϕ and 30° over the elevation angle at the horizontal plane for urban channel. For suburban channel the variation over elevation angle is similar to urban channel where as the azimuth will have laplacian spectrum distribution of various $\sigma_\phi = 5°$, 10°, 15° and 20°.

The E_ϕ and E_θ of the incident fields were assumed independent over all angles of θ and ϕ, and their variations are uniform over the channel properties under considerations. It was also assumed that the phase variations are uniform over 0 to 2π.

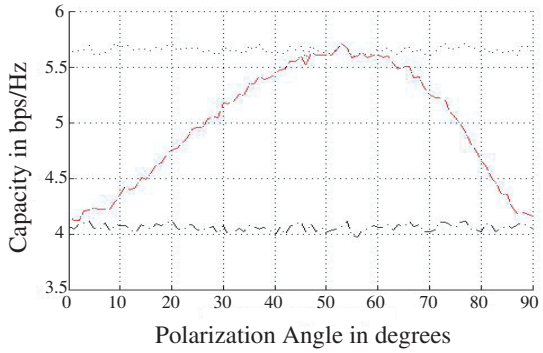

Figure 2: The channel capacity of 2×2 MIMO system as oriented in Figure 1 as a function of the polarization angle. ('. . . ': upper limit of 2×2 MIMO fading channel, '.-.-.-': upper limit of 2×1 MIMO fading channel, Capacity using Eq. 1: red line, Capacity using Eq. 15: blue dots).

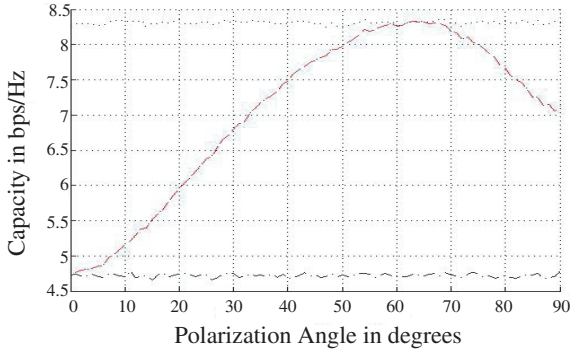

Figure 3: The channel capacity of 3×3 MIMO system as oriented in Figure 1 as a function of the polarization angle. ('. . . ': upper limit of 3×3 MIMO fading channel, '.-.-.-': upper limit of 3×1 MIMO fading channel, Capacity using Eq. 1: red line, Capacity using Eq. 2: blue dots).

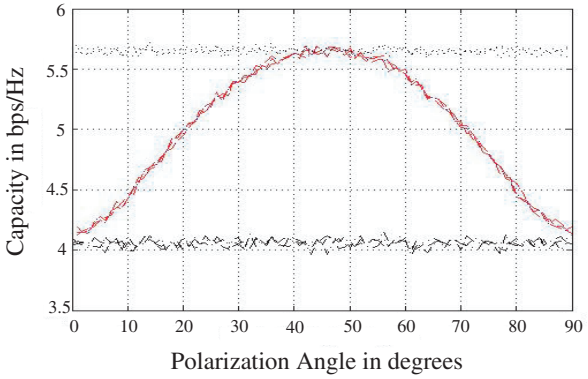

Figure 4: The channel capacity of 2×2 MIMO system as oriented in Figure 1 (the antennas are rotated by 90 degrees over azimuth angle) as a function of the polarization angle. ('. . . ': upper limit of 3×3 MIMO fading channel, '.-.-.-': upper limit of 3×1 MIMO fading channel, Capacity using Eq. 1: red line, Capacity using Eq. 2: blue dots). The elevation angle is varied uniformly over 30 degrees at the horizontal plane, whereas azimuth angle varied as Laplacian spectrum of different values of σ_ϕ $(5, 10, 15, 20$ degrees for the geometry presented in Figure 1) in which the azimuth direction randomly selected between 0 and 2π.

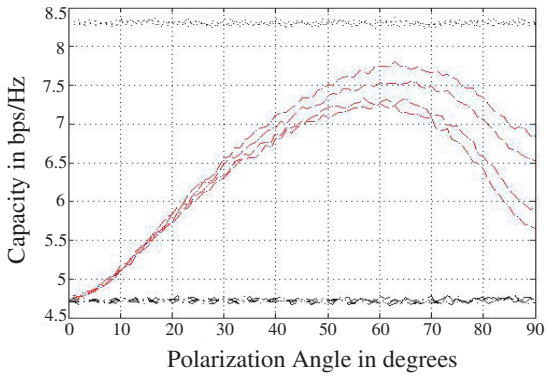

Figure 5: The channel capacity of 3×3 MIMO system as oriented in Figure 1 (the antennas are located at 90, 210 and -30 azimuth angles) as a function of the polarization angle. ('. . . ': upper limit of 3×3 MIMO fading channel, '.-.-.-': upper limit of 3×1 MIMO fading channel, Capacity using Eq. 1: red line, Capacity using Eq. 2: blue dots). The elevation angle is varied uniformly over 30 at the horizontal plane, whereas azimuth angle varied as Laplacian spectrum of different values of σ_ϕ $(5, 10, 20, 30$ degrees for the geometry presented in Figure 1) in which the azimuth direction randomly selected between 0 and 2π.

Channel capacity of 2×2 MIMO and 3×3 MIMO systems for urban channel are shown in Figures 2 and 3. The antennas for 2×2 MIMO are located at $\phi = 0°$ and $\phi = 180°$ where as

for 3×3 MIMO at $\phi = 0°$, $120°$ and $240°$. In these figures a closed form solutions of the W_r are found and then the capacity was evaluated under Raleigh channel in which the average was taken over 1000 complex samples and in each point the transfer function was normalized to have a good prediction of the maximum variation of the spatial matrices using these types of antennas. It is simply can be noticed that the maximum capacities for 2×2 MIMO and 3×3 MIMO occur at around $55°$ and $63°$. These angles are recommended to represent the othogonalities of the spatial fields required by the antennas given in Figure 1.

Similarly, for Suburban channel the capacity of 2×2 and 3×3 MIMO system are shown in Figures 4 and 5 respectively for various values of σ_ϕ. It should be noted that the maximum capacity limits for 2×2 MIMO channel were achieved for all values presented for σ_ϕ where as for the 3×3 MIMIO were slightly reduced as σ_ϕ is increasing.

Basically, the MIMO channel capacity for different transmitted power is shown in Figure 6. In this example the variations of the elevation angle is considered between $\theta = 0$ to π where as in azimuth are similar to that presented in Figures 2 and 3. It is clearly the maximum capacities are proportional linearly with the transmitted power in which the maximum location for each transmitted power is fixed at around $63°$.

Figure 7 demonstrates the capacity variations for urban channel using ring array of three elements. The channel capacity was reached when the ring radius was about $\lambda/4$ (i.e., the separated distance between the radiating elements was around $\lambda/2$). Comparing the antenna sizes in Figures 1 and 7, it is evidence that the spatial polarization diversity has the ability to achieve the maximum capacity with certain constraints on the field orthogonalites.

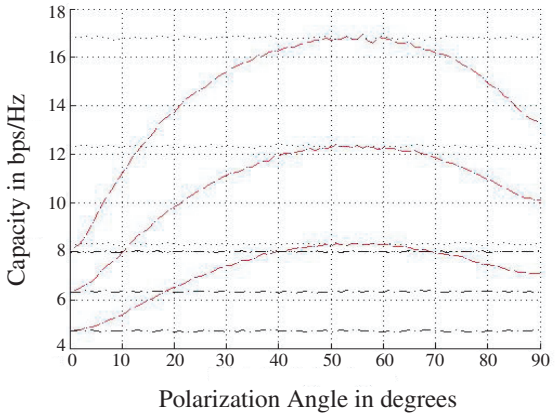

Figure 6: The channel capacity of 3×3 MIMO system as oriented in Figure 1 as a function of the polarization angle for different SNR starting from 10 dB, 15 dB and 20 dBs. ('. . . ': upper limit of 3×3 MIMO fading channel, '.-.-.-': upper limit of 3×1 MIMO fading channel, Capacity using Eq. 1: red line, Capacity using Eq. 2: blue dots). The elevation angle is varied uniformly over 180 degrees at the horizontal plane.

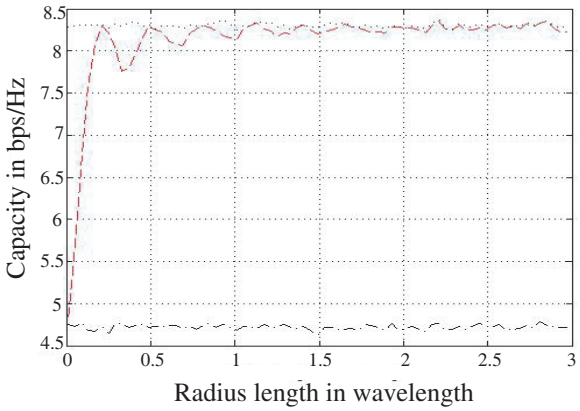

Figure 7: The channel capacity of 3×3 MIMO system as oriented on a ring (the antennas are located at $0, 120$ and -120 azimuth angles) as a function of the radius distance in wavelength (c). ('. . . ': upper limit of 3×3 MIMO fading channel, '.-.-.-': upper limit of 3×1 MIMO fading channel, red line, Capacity using Eq. 2: blue dots).

4. CONCLUSIONS

The channel capacity of a simple 2×2 and 3×3 MIMO systems using spatial polarization diversity was presented for different channel assumptions. The presented results show that the maximum channel capacity within small volume space can be reached with careful selection of the spatial field's orthonoalities. The results also compared to planner array MIMO system operation in which the antenna size considered was much larger to the MIMO system presented here. However, the work is still in progress to include the mutual coupling between the antennas and implementation on the mobile handset.

REFERENCES

1. Foschini, G. J. and M. J. Gans, "On limits of wireless communication in a fading environment when using multiple antennas," *Wireless Personal Commun.*, Vol. 6, No. 3, 311–335, Mar. 1998.
2. Foschini, G. J. and R. A. Valenzuela, "Initial estimation of communication efficiency of indoor wireless channel," *Wireless Networks*, Vol. 3, 141–154, 1997.
3. Wallace, J. W. and M. A. Jensen, "Modeling the indoor MIMO wireless channel," *IEEE Trans. Antennas Propag.*, Vol. 50, No. 5, 591–599, May 2002.
4. Wallace, J. W., M. A. Jensen, A. L. Swindlehurst, and B. D. Jeffs, "Experimental characterization of the MIMO wireless channel: Data acquisition and analysis," *IEEE Trans. Wireless Commun.*, Vol. 2, No. 2, 335–343, Mar. 2003.
5. Gesbert, D., H. Bölcskei, D. A. Gore, and A. Paulraj, "Outdoor MIMO wireless channels: Model and performance prediction," *IEEE Trans. Commun.*, Vol. 50, No. 12, 1926–1934, Dec. 2002.
6. Dong, L., H. Choo, R. W. Heath, and H. Ling, "Simulation of MIMO channel capacity with antenna polarization diversity," *IEEE Trans. Wireless Commun.*, Vol. 4, No. 4, 1869–1873, Jul. 2005.
7. Winters, J. H., J. Salz, and R. D. Gitlin, "The impact of antenna diversity on the capacity of wireless communication systems," *IEEE Trans. Commun.*, Vol. 42, 1740–1751, Feb. 1994.
8. Andrews, M. R., P. P. Mitra, and R. deCarvalho, "Tripling the capacity of wireless communications using electromagnetic polarization," *Nature*, Vol. 409, No. 6818, 316–318, Jan. 2001.
9. Svantesson, T., "On capacity and correlation of multi-antenna systems employing multiple polarizations," *IEEE Int. Antennas Propagation Symp. Digest*, 202–205, San Antonio, TX, Jun. 2002.
10. Stancil, D. D., A. Berson, J. P. Van't Hof, R. Negi, S. Sheth, and P. Patel, "Doubling wireless channel capacity using co-polarised, co-located electric and magnetic dipoles," *Electron. Lett.*, Vol. 38, No. 14, 746–747, Jul. 2002.
11. Andersen, J. B. and B. N. Getu, "The MIMO cube—A compact MIMO antenna," *5th Int. Symp. Wireless Personal Multimedia Communications*, 112–114, Honolulu, HI, Oct. 2002.
12. Xu, H., M. J. Gans, N. Amitay, and R. A. Valenzuela, "Experimental verification of MTMR system capacity in controlled propagation environment," *Electron. Lett.*, Vol. 37, No. 15, 936–937, Jul. 2001.